Computers, Environment and Urban Systems 105 (2023) 102027

Contents lists available at ScienceDirect

Computers, Environment and Urban Systems

journal homepage: www.elsevier.com/locate/ceus

Detecting older pedestrians and aging-friendly walkability using computer vision technology and street view imagery

Dongwei Liu[a], Ruoyu Wang[b], George Grekousis[c], Ye Liu[c], Yi Lu[a,*]

[a] Department of Architecture and Civil Engineering, City University of Hong Kong, Hong Kong
[b] Centre for Public Health, Queen's University Belfast, Belfast, Northern Ireland, United Kingdom
[c] School of Geography and Planning, Sun Yat-Sen University, Guangzhou, China

ARTICLE INFO

Keywords:
Walkability
Aging friendly
Street view imagery
Human attributes recognition
Transfer learning
Walking
Pedestrian demand

ABSTRACT

As an emerging and freely available urban big data, Street View Imagery (SVI) has proven to be a useful resource to examine various urban phenomena in human behavior, the built environment and their interactions. However, due to technical limitations, previous studies often focused on general pedestrians and ignored certain population subgroups such as older adults. In this study, we develop an innovative method for detecting older pedestrians using SVI. We adopted transfer learning to train a model which can accurately detect older pedestrians on SVI with an accuracy of 87.1%.

Using Hong Kong as a case study, we created a dataset consisting of 72,689 street view panoramas and detected 7763 older pedestrians and 29,231 non-older pedestrians. We further visualized the distribution of detected older pedestrians and found a significant spatial discrepancy between older pedestrians and residential population of older adults. To account for this spatial discrepancy, this study proposed a novel index to assess pedestrian demand and walking environment based on the ratio of the number of pedestrians and the residential population. We also found pedestrian demand assessed with this index has a stronger correlation with the built environment compared with population-level travel survey. This novel approach can be used to assess pedestrian demand for older adults, as well as aging-friendly walking environment.

1. Introduction

With rapidly aging populations in many countries, more and more governments and researchers have recognized the importance of building age-friendly cities. Researchers have found that regular physical activities can significantly increase older adults' life expectancy (Lee et al., 2012) and reduce the risk of having chronic diseases such as cardiovascular disease (Smith, Wingard, Smith, Kritz-Silverstein, & Barrett-Connor, 2007), coronary heart disease (Manson et al., 1999), type 2 diabetes (Aune, Sen, Henriksen, Saugstad, & Tonstad, 2016), breast cancer (Wu, Zhang, & Kang, 2013), and colon cancer (Boyle, Keegel, Bull, Heyworth, & Fritschi, 2012). As the most common form of physical activity among older adults, walking has therefore attracted considerable attention (Chodzko-Zajko et al., 2009; Pahor et al., 2014). Due to their declined physical abilities and mobility associated with aging, older adults are more sensitive to the surrounding built environment than young adults (Chen, Lu, Ye, Xiao, & Yang, 2022; Feng, 2017; Ghani, Rachele, Loh, Washington, & Turrell, 2018), so it is important to investigate walking environment for older adults.

Researchers often employed walkability to assess the walking environment, which is defined as the synergy of certain built environmental factors, including density, diversity, and design, which can promote and support walking (Forsyth, 2015). For example, the World Health Organization (WHO) has summarized 88 essential indicators for evaluating aging-friendly cities, of which 12 features relate to the built-environment factors for pedestrians (Organization, W. H, 2007). Some researchers used the Walk Score, a rating system calculated based on the distance to the nearest amenities such as hospitals and schools, to measure walkability (Carr, Dunsiger, & Marcus, 2010). However, these measurements focus only on the availability of walkable infrastructure and walking opportunities, and may not reflect actual pedestrian demand on streets (Chen et al., 2020; Dhanani, Tarkhanyan, & Vaughan,

* Corresponding author at: Department of Architecture and Civil Engineering, City University of Hong Kong, 83 Tat Chee Avenue, Kowloon Tong, Kowloon, Hong Kong Special Administrative Region.

E-mail addresses: dongweliu3-c@my.cityu.edu.hk (D. Liu), r.wang@qub.ac.uk (R. Wang), graikousis@mail.sysu.edu.cn (G. Grekousis), liuye25@mail.sysu.edu.cn (Y. Liu), yilu24@cityu.edu.hk (Y. Lu).

https://doi.org/10.1016/j.compenvurbsys.2023.102027
Received 22 April 2023; Received in revised form 8 August 2023; Accepted 11 August 2023
Available online 19 August 2023

2017) An area with high walkability may not necessarily have higher pedestrian activity, and similarly, an area with low walkability may still have many pedestrians.

Indeed, the association between built environment factors and walking behavior tends to be intertwined and dependent on the social and urban context. For example, higher urban density often promotes walking behavior in low or medium-density cities. However, such association tends to be insignificant in high-density cities such as Hong Kong (Cerin et al., 2013; Kamada et al., 2011). Additionally, empirical studies have found that the walking behaviors of disadvantaged populations tend to be less responsive to built-environment factors, and even demonstrate opposite responses to the expected effects of these factors (Adkins, Makarewicz, Scanze, Ingram, & Luhr, 2017; Forsyth, Oakes, Lee, & Schmitz, 2009; Frank, Kerr, Sallis, Miles, & Chapman, 2008; Huang, Li, Yu, Yang, & Wang, 2022; Lovasi, Quinn, Neckerman, Perzanowski, & Rundle, 2008). Therefore, it is also important to obtain pedestrian demand on streets (Chen et al., 2020). This approach may arguably be more accurate and straightforward to assess pedestrian activity than walkability-based methods.

There are two common approaches to collect fine-grained pedestrian demand data. The first is field observation (Brownson, Hoehner, Day, Forsyth, & Sallis, 2009). But it is costly, time-consuming and inefficient. The second approach is to infer pedestrian activity from population-level travel surveys (Schwartz, 2000). However, such inferring may be inaccurate because people tend to underreport short walking trips or short walking legs of a trip (Chen et al., 2022). In recent years, researchers have begun using Street View Imagery (SVI) and computer vision techniques to estimate pedestrian volume in a large area such as a whole city, because of its efficiency and cost-effectiveness. However, due to technical limitations, most existing research only uses SVIs to detect pedestrians, but not to classify pedestrians by age (Chen et al., 2020; Yin, Cheng, Wang, & Shao, 2015).

Therefore, the main purpose of this study is to develop a novel method to detect older pedestrians using SVI and a non-facial human attributes recognition algorithm. We also analyze the spatial distribution of older pedestrians in a whole city. This study contributes to existing knowledge in four aspects. First, we established a large SVI-based dataset with labels for older pedestrians. Second, we developed a novel method for detecting older pedestrians using SVI and a non-facial human attributes recognition approach. Third, we examined the spatial distribution of older pedestrians in an entire city. Fourth, we used the ratio of the detected pedestrians and the number of residents to evaluate walking environment.

2. Related works

2.1. Measurement walking behaviors of older adults

Although numerous studies focus on walking behavior and other physical activities of older adults, most of them have concentrated on North America and Europe where older people have different lifestyles and walking habits compared to East Asia. For example, North American and European studies (Bennie et al., 2013; de Rezende et al., 2014; Harvey, Chastin, & Skelton, 2015) found that older adults spent less time on walking compared with younger people, while Asian (Hong Kong and Japan) studies found the opposite outcomes (Hui, Chan, Wong, Ha, & Hong, 2001; Tsunoda et al., 2012). The methods to measure walking behaviors also differ across studies. Most studies focus on the individual walking behavior (IWB) of older people, such as daily walking time, walking frequency, and walking distance (Mendes de Leon et al., 2009; Moniruzzaman, Páez, Scott, & Morency, 2015; Shigematsu et al., 2009; Van Holle et al., 2016). Some studies focus on collective walking behavior (CWB) such as urban vitality and pedestrian volume (Chen et al., 2020; Lee, Sung, & Woo, 2017; Sung, Lee, & Cheon, 2015). Traditionally, IWB can be obtained by questionnaire (Barnett, Barnett, Nathan, Van Cauwenberg, & Cerin, 2017) while CWB can be assessed by field observation (Yin, 2017). However, these approaches are costly, time-consuming, and unsuitable for large-scale studies. Recently, researchers employed urban big data such as smart card data (Long & Thill, 2015) and mobile signal data (Du, Yue, Ji, & Sun, 2017) to assess both IWB and CWB. However, such data still cannot differentiate street-level pedestrian behaviors, because such data sources tend to have low spatial resolution (e.g., 10 m or 100 m).

2.2. SVI as a novel data to measure urban environment and walking activity

The recent proliferation of Street View imagery (SVI), rapid advances in computer vision technology and soaring computing power have created great opportunities for measuring street-level built-environment and human activities. Some researchers focused on auditing features of the urban environment such as buildings (Ogawa & Aizawa, 2019), street greenery (Liu, Jiang, Wang, & Lu, 2023; Lu, 2019), and sidewalks (Ning, Ye, Chen, Liu, & Cao, 2022), while the others used SVIs to predict people's subjective perception of the urban environment such as safety (Wang et al., 2019) and aesthetics (Luo, Xie, & Furuya, 2022).

On the other research front, some researchers have begun to use SVIs to directly quantify pedestrian volumes. For example, some researchers have started to pay attention to the potential of SVIs to assess pedestrian volume. Yin et al. (2015) developed an approach to automatically extracting pedestrian counts on Google SVIs using deep learning technology. They validated the reliability of the proposed method across 200 street segments in Buffalo, NY, Washington, D.C., and Boston, MA, USA, and found it can produce consistent results with both manual count with Google SVIs and field count. Chen et al. (2020) has further validated the robustness of using SVIs to estimate pedestrian volume over 700 street segments in Tianjin, China, by comparing with field observation data (Chen, Wang, Bao, & Lou, 2022).

2.3. Non-facial human attributes recognition (NHAR) and crowd analysis

Non-facial human attributes recognition (NHAR) which aims to recognize, describe, and understand human attributes from images without facial information, has attracted much attention in computer vision field in recent years (Wang et al., 2022). The face is the most distinctive part of humans and provides an invaluable data source for computer vision algorithms (Thom & Hand, 2020). However, human faces in SVIs are intentionally blurred to protect privacy (Deng, Luo, Loy, & Tang, 2014). Therefore, it is necessary to detect human attributes from non-facial human parts, such as whole body (Hidayati, You, Cheng, & Hua, 2017) or clothing (Xiang, Dong, Pan, & Gao, 2020). Pedestrian attributes recognition (PAR) (Wang et al., 2022) is one such emerging technique with promising results. It mainly relies on data derived from people's posture and gestures. Existing studies have shown that PAR along with transfer learning (Weiss, Khoshgoftaar, & Wang, 2016) and data augmentation (Shorten & Khoshgoftaar, 2019) can efficiently recognize many different human attributes from images.

Because some pedestrians walk in groups, detecting individuals from a large group of pedestrians presents additional technical challenges. A new technique known as crowd analysis, may address this issue (Wu, Moore, & Shah, 2010). Crowd analysis is usually applied in crowd behavior analysis (Saxena, Brémond, Thonnat, & Ma, 2008), people counting (Liang, Zhu, & Wang, 2014), anomaly detection (Husni & Suryana, 2010) and people tracking (Rodriguez, Laptev, Sivic, & Audibert, 2011). Recently, it has been used for pedestrian detection and pedestrian volume estimation based on SVIs (Chen et al., 2020; Yin et al., 2015).

3. Methodology

3.1. Study area

As one of the densest and most urbanized cities in the world, Hong Kong houses >7 million residents in a land of only 1100 km^2. Hong Kong also witnesses an increasingly aging population, presenting various challenges for the region. The number of older adults aged 65 and over is expected to increase from 1.45 million (19.1% of the total population) in 2021 to about 2.37 million (31.1%) in 2036 (Census and Statistics Department, 2020). According to the government, Hong Kong will become one of the cites with the highest percentage of older residents in the world by 2050 (Census and Statistics Department, 2020). In this study, we selected the whole Hong Kong region as our study area and focus on all streets covered by Google Street View (Fig. 1).

The entire territory of Hong Kong consists of three parts: Hong Kong Island, Kowloon and the New Territories. The dense urban region in Hong Kong is centralized on Hong Kong Island and Kowloon, which collectively cover a mere 13.8% of the total area, yet house 50% of the population. Conversely, the New Territories predominantly comprise country parks and rural areas, but with over 3 million population concentrated in new towns. On Google Maps, there are 70,021 SVI sample points for the entire Hong Kong area, covering 31,971 street segments and 199 Tertiary Planning Units (TPUs). Among them, 11,467 SVI sample points were detected to have pedestrians.

3.2. The overall study design

Fig. 2 shows the overall workflow of older pedestrian detection and data analysis. First, we detected and cropped pedestrians from SVIs for the entire Hong Kong area using the pre-trained You Only Look Once (YOLO) v5x6 model (Redmon & Farhadi, 2017). Then, we classified these pedestrians into two groups (non-elderly vs. older adults) using Resnet50. Resnet50 was pre-trained with the modified dataset RAP and PA -100 K and fine-tuned labeled SVIs. In this way, we obtain the pedestrian volume with age information for each street in Hong Kong covered by SVIs.

3.3. Dataset for model training

3.3.1. Pretraining dataset

To improve the accuracy of the model, we used the Richly Annotated Pedestrian dataset (RAP) (Li, Zhang, Chen, & Huang, 2018) and the PA -100 K (Liu et al., 2017) dataset for pretraining. RAP (Richly Annotated Pedestrian) and PA-100 K are datasets specifically curated for human attribute recognition, and person re-identification tasks in computer vision research. These datasets are generally designed for academic research and are meant to facilitate training and benchmarking deep learning.

RAP dataset contains 41,585 pedestrian images captured by surveillance cameras in various public places like streets, parks, and shopping malls. The images come from the CASIA Office of Turing Robotic Intelligence and the Harbin Institute of Technology in China. The dataset is richly annotated with various pedestrian attributes such as age, gender, clothing, accessories, and occlusions.

PA-100 K dataset consists of 100,000 pedestrian images, making it one of the largest and most comprehensive pedestrian attribute recognition datasets. The images were collected from multiple sources, including surveillance cameras from many countries worldwide. Although specific countries are not explicitly mentioned, it is safe to assume that the dataset maintains diversity in terms of ethnicity, clothing, and backgrounds. It is annotated with 26 attributes like gender, age, clothing type, hairstyle, and accessories.

We combined these two datasets into one. Each image contains a person tagged with multiple tags, including age and gender. Age in RAP and PA -100 K was divided into five classes, including <16, 16–30, 31–45, 46–60, and over 60 years old. In this study, we focused on pedestrians who are over 60 years old, so we combined the other four classes into one class: 60 years old or less. The final combined dataset contains 1654 images with older adults and 1654 images with others. To avoid imbalance between the number of images with older adults and people in other age groups, we selected all 1654 images with older adults and randomly selected 1654 images with people in other age groups from the combined dataset. We then performed data augmentation on these two newly selected datasets (NSD).

Since each pedestrian in SVIs is face masked, we masked the same areas of the images in RAP and PA -100 K to reduce the difference between the training dataset and the target dataset (Fig. 3).

3.3.2. SVIs dataset for fine-tuning

Pedestrians in SVIs have different distortions, distributions, and background information that do not match RAP and PA -100 K. To fit the classification model to the context of SVIs, a fine-tuning process for the pre-trained model is needed. We downloaded SVIs for all sample points

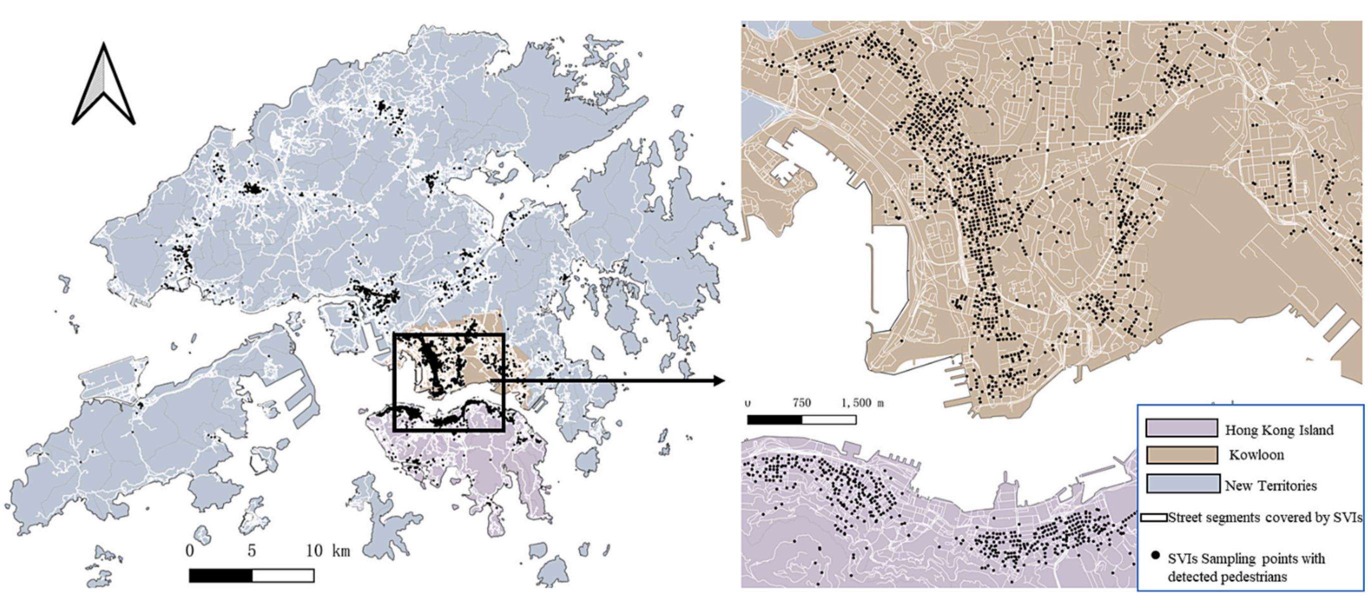

Fig. 1. The area of Hong Kong region and the distribution of SVI sampling sites. There are 70,021 SVIs and 11,467 of them have detected pedestrians.

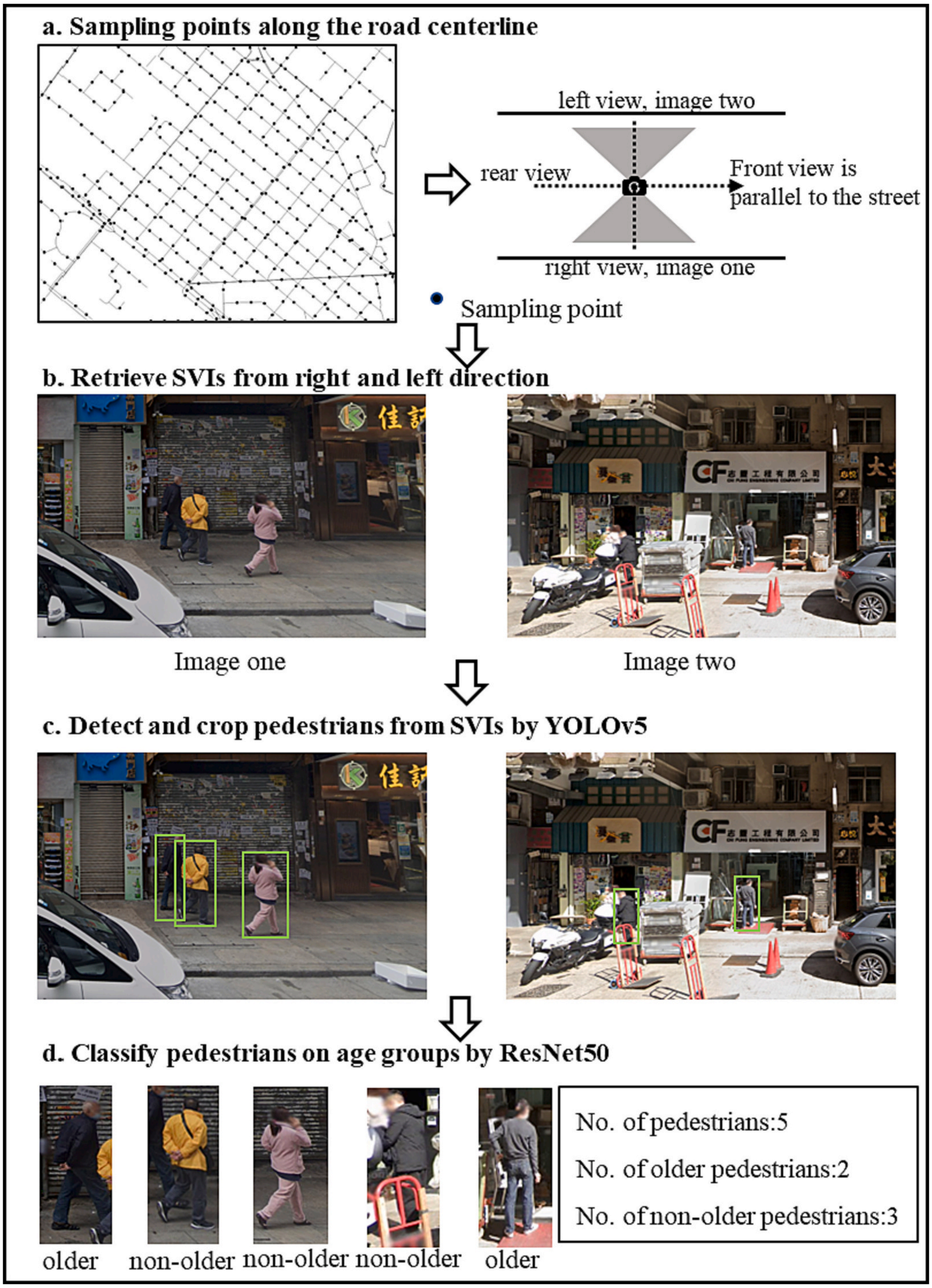

Fig. 2. Workflow of the proposed model. (a) Sampling points along the road centerline; (b) Retrieve SVIs from right and left direction; (c) Detect and crop pedestrians from SVIs by YOLOv5; (d) Classify pedestrians on age groups by ResNet50.

in Hong Kong from Google Street View, maintaining a 50-m separation between each pair of sampling locations. Each sample point has four SVIs with a direction of 0°, 90°, 180°, and 270°. All downloaded images have a size of 1024*1024 pixels and were taken between 2018 and 2019. From them, we selected 2000 SVIs in different scenes (downtown, suburban, highway, etc.) to create a dataset for fine-tuning. Three trained research assistants participated in pedestrian labeling. Two of them performed the labeling while the third one reviewed their results. In SVIs, each pedestrian's face is masked, so we determined age based on features other than the face. If a pedestrian has obvious aging characteristics such as white hair and a strong hunchback, he or she is classified as an older adult. Accurately determining the ages of pedestrians remains challenging. Therefore, our research assistants only classify them based on their perceived age group, differentiating between older and non-older adults without specifying their precise age. We also discarded the pedestrians 50-m away from a SVI sampling point because it is challenging to classify age group with a small image. Finally, a total of 1546 pedestrians were labeled, including 708 older adults and 838 non-older individuals (Fig. 4).

Fig. 3. (a), (b), (c) are non-older pedestrian masked with face in RAP and PA-100 K, and (d), (e) are older pedestrian masked with face in RAP and PA-100 K.

Fig. 4. (a), (b), (c) are non-elderly in SVI, and (d), (e) are older adults in SVI.

3.4. Detector and classifier

The target of the object detection model used in this study is to detect pedestrians from SVIs and classify them into two age groups. Object detection models can be divided into two types based on their pipelines. One is one-stage models, such as You Only Look Once (YOLO) series (Redmon, Divvala, Girshick, & Farhadi, 2016) and single shot multibox detector (SSD) (Liu et al., 2016). The other is two-stage models, which segregates detection and classification processes, such as Faster R-CNN, which offers better performance than one-stage models (Ren, He, Girshick, & Sun, 2015). In this study, we performed the detection and classification process separately to improve the performance of the model. First, we used the pre-trained YOLO v5x6 (Redmon & Farhadi, 2017) to detect pedestrians from SVIs and cropped them down. The 0.5mAP (mean average precision at IoU 0.5) for the pretrained YOLO v5x6 to detect pedestrians in SVIs is 87.7. Next, we classified the cropped pedestrians with our best fitted model. After our pilot study, we found that Resnet50 (Koonce, 2021) offered the best tradeoff in terms of classification performance, run-time, and memory consumption.

3.4.1. YOLO model

As the most popular one-step object detection model series, YOLO series has outperformed other object detection models in terms of accuracy and speed. The YOLO series also has advantages in detecting objects of different sizes and overlapping objects. In terms of effectiveness and stability, we selected YOLO v5, the fifth versions of YOLO series, as the detector for our approach. From the YOLO v5 family, we selected the YOLOv5x6 model with the largest size, which was pretrained on the COCO dataset (Lin et al., 2014) and achieved 72.0 0.5mAP for the validation dataset.

The basic architecture of YOLOv5 is shown in Fig. 5. The whole network consists of five sections: Input, Backbone, Neck, Head, and Output. The backbone section functions as the feature extractor and transfers input images into feature maps. The neck section receives feature maps from the backbone and combines these features into logic groups for detection. The head section is also called the detection section. It outputs vectors containing the probability for each class, the position and the size of each object.

3.4.2. Resnet 50 model

Classifying pedestrian age groups from SVIs requires deep CNN due to high intraclass variance and low interclass variance. Training deep neural networks is challenging due to the vanishing gradient problem (Habibzadeh, Jannesari, Rezaei, Baharvand, & Totonchi, 2018) and the degradation problem (Wichrowska et al., 2017). To address these challenges, the Residual Network (ResNet) was developed. The

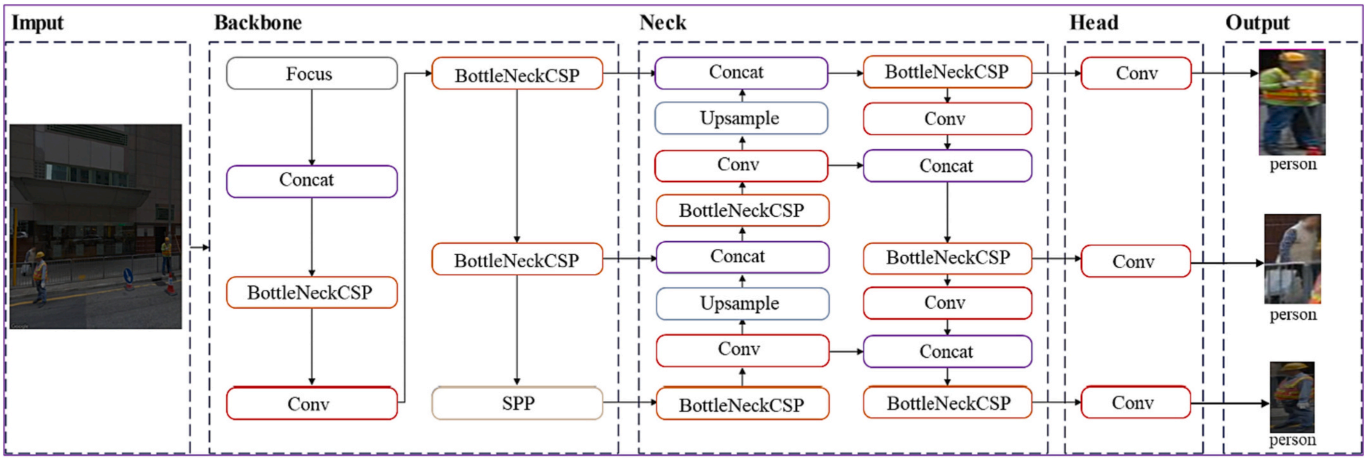

Fig. 5. Overview of the architecture of YOLO v5.

fundamental part of ResNet is batch normalization. Batch normalization modifies the input layer to improve the performance of the network and reduce the shifting of covariates. Another key area is identity connectivity, which helps ResNet's network mitigate the vanishing gradient problem.

In this study, we used the ResNet50 (Fig. 6), which is a variant of ResNet model and can handle the input images with height, width as multiple of 32 and 3 as channel width. The output of ResNet50 is the probability of each class, and we selected the class with higher probability as the classified result for each pedestrian cropped from SVIs.

Table 1
Comparison of model performances through different training dataset.

Models	Attribute	Training dataset	Test dataset	Highest accuracy
Resnet50	Older adult	Cropped SVIs	Cropped SVIs	82.2%
Resnet50	AgeAbove60/ Older adult	RAP and PA-100 K	Cropped SVIs	76.8%
Resnet50	AgeAbove60/ Older adult	RAP and PA-100 K/Cropped SVIs	Cropped SVIs	87.1%

3.5. Model training and evaluation

First, we randomly split the NSD dataset: 75% for training dataset, 25% for validation. Second, we employed YOLO v5x6 to crop each pedestrian from labeled SVIs to create our customized dataset. Third, we again randomly split the customized data: 70% for training, 20% for validation, and 10% for test.

Next, we conducted three groups of experiments. In the first group, we trained models with only NSD dataset. In the second group, we trained models with only the training and the validation dataset of customized SVIs. In the third group, we pretrained the models using the NSD dataset and fine-tuned models with training and validation dataset of customized SVIs. All three groups of models are tested by the test dataset of customized SVIs. The results of the three groups of experiments are shown in Table 1. The result showed that the model pretrained in the NSD and fine-tuned in cropped SVIs performed the best with an accuracy of 87.1%. Please note that the age categorization of cropped SVIs is determined by research assistants based on their perceived age group. It only differentiates between older and non-older adults without specifying their precise age. In this study, the attribute of AgeAbove60 in NSD is aligned with the classification of older adult in Cropped SVIs.

4. Pedestrian detection and recognition in Hong Kong

4.1. Geographic distribution

The final trained model detected 35,353 pedestrians from 70,021 SVIs in Hong Kong, including 7375 older pedestrians and 27,978 non-older pedestrians. We mapped and visualized the number of detected

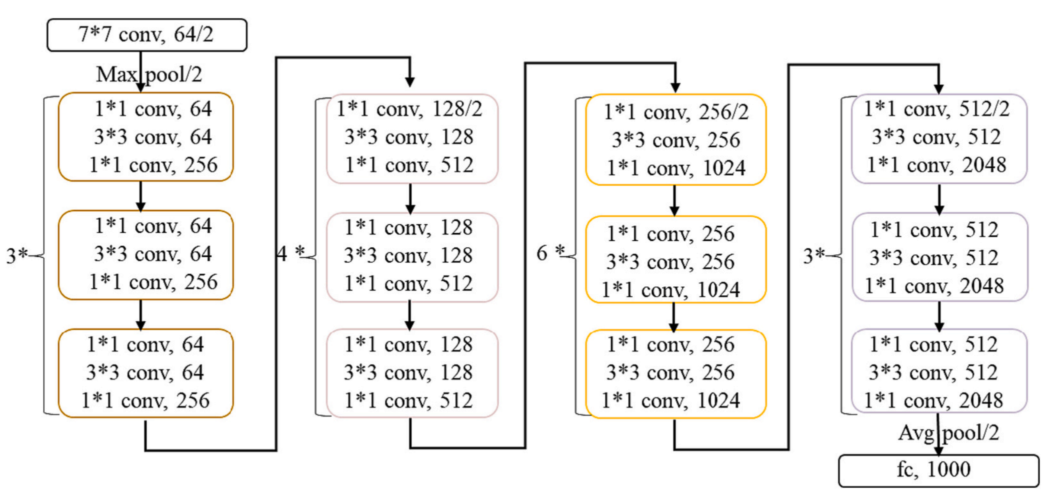

Fig. 6. Overview of the architecture of ResNet50.

older pedestrians and the proportion of older pedestrians among all detected pedestrians within different spatial units in Hong Kong.

More older pedestrians were detected in dense urban areas of Kowloon and Hong Kong Island (Fig. 7a and b). In terms of proportions, a high proportion of older pedestrians among all pedestrians were found in TPUs distributed around Hong Kong Island and new towns in New Territories (Fig. 7c and d).

4.2. Spatial mismatch between older pedestrians and older residents

To analyze any potential spatial mismatch between detected older pedestrians and older residents, we conducted two comparative analyses. We collected resident population in a specific area in 2020 from WorldPop (worldpop.org). This dataset estimates population residing in each 100 m*100 m grid using census data in 2020 and a random forest model (Stevens, Gaughan, Linard, & Tatem, 2015). In urban areas, a walk of 500 m or less to the nearest amenity is a desirable distance, so researchers typically use 500-m square grids to study walking behavior and walkability (Dovey & Pafka, 2020). Therefore, we aggregated the data of both detected pedestrians and WorldPop into 500 m* 500 m square grid.

First, we compared the number of detected older pedestrians and the population of older residents in each grid. We classified all grids with high or low (H or L) values of detected older pedestrians and older residents, according to the median value of the two variables respectively. Accordingly, we classified the grids into four groups: H/H (high number of older pedestrians and high population of older residents), H/L, L/H, and L/L (Fig. 8 and Tables 2 & 3). In Table 3, we conducted *t*-tests on built environment factors for four pairs of comparisons (H/H grids vs. non-H/H grids, L/H vs. non-L/H, H/L vs. non-H/L, L/L, vs. non-L/L in Fig. 8).

H/H grids are mainly located in high density residential area of Kowloon and Hong Kong Island such as Sham Shui Po, Yau Ma Tei, and new developed town centers in New Territories. They have higher population density and proportion of residential area, and shorter distance to MTR station and to city center, compared with other grids. L/H grids are mainly concentrated in major commercial hubs or mixed used areas such as Tsim Sha Tsui, Central District. They have higher

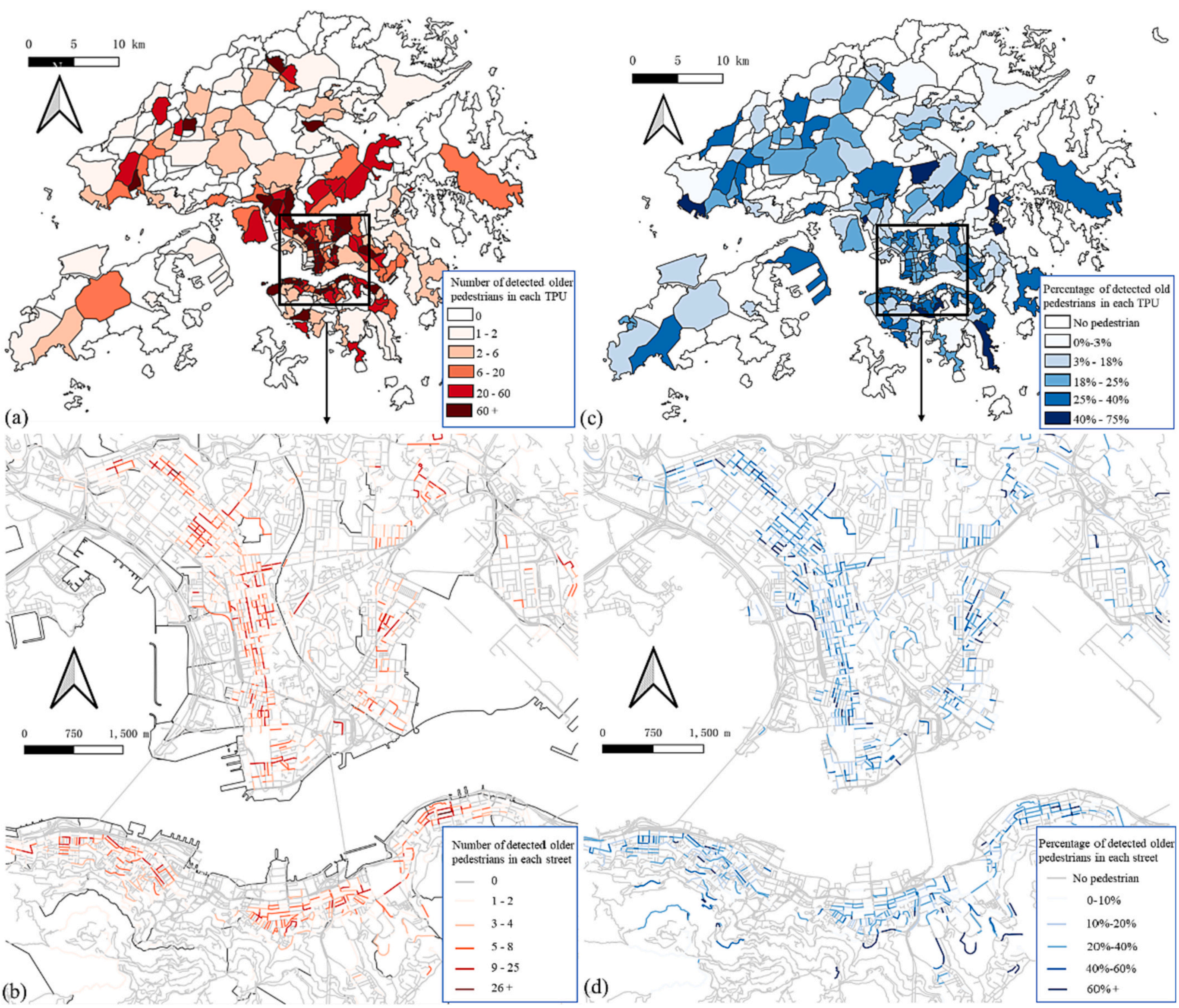

Fig. 7. The geographic distribution of detected older pedestrians in Hong Kong. (a) number of older pedestrians in TPUs; (b) number of older pedestrians in road segments in the core urban area (including most part of Hong Kong Island and Kowloon); (c) the proportion of older pedestrians among all detected pedestrians in TPUs; (d) the proportion of older pedestrians among all detected pedestrians in road segments in the core urban area.

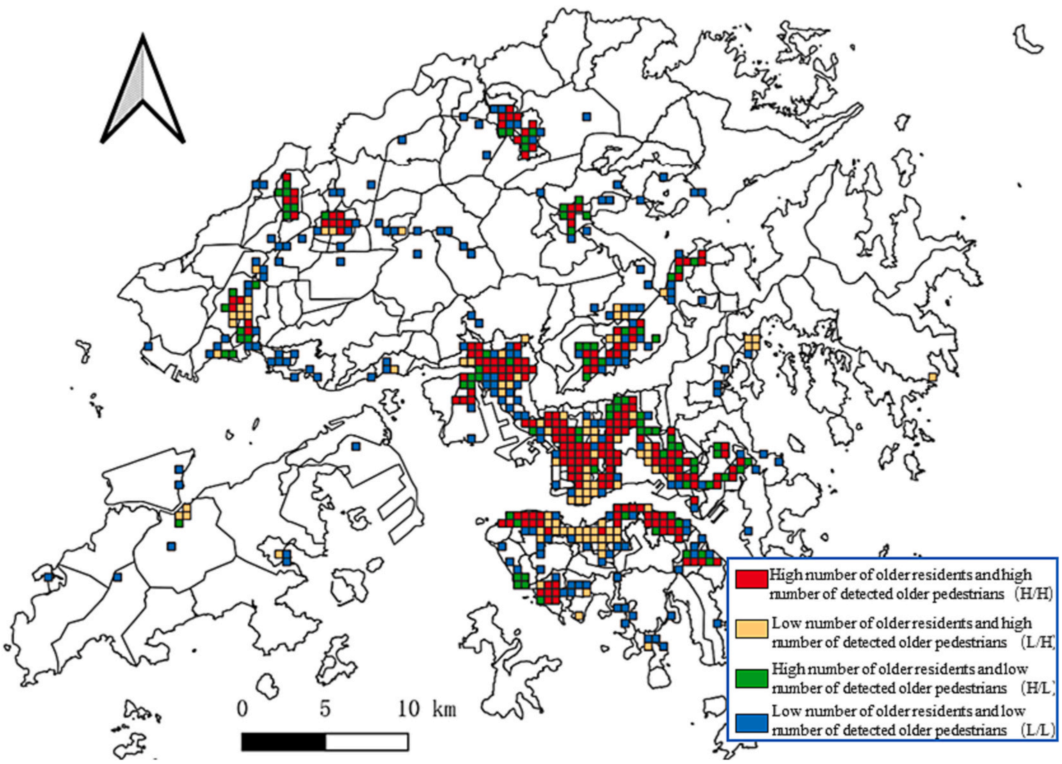

Fig. 8. Classification of urban areas into four groups, according to the population of older residents and the number of detected older pedestrians on SVIs.

Table 2
Features and representative examples of four groups of areas in Fig. 8.

Type of area	Features	Representative location	Representative aerial view
High number of older residents and high number of detected older pedestrians (H/H)	High density residential area	Sham Shui Po, Yau Ma Tei	
Low number of older residents and high number of detected older pedestrians (L/H)	High density commercial & mixed used area	Tsim Sha Tsui, Central District	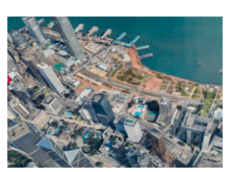
High number of older residents and low number of detected older pedestrians (H/L)	Medium density residential area	Waterfall Bay, Tsing Shan Tsuen	
Low number of older residents and low number of detected older pedestrians (L/L)	Suburban and mountainous area	Stanley, Sai Wan Shan, Yau Tong	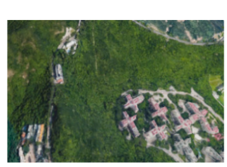

Source: Google Inc.

proportion of commercial area, lower population density and proportion of residential area, and shorter distance to city center. H/L grids are mainly located in residential areas (e.g., Waterfall Bay, Tsing Shan Tsuen) scattering in the perimeter of H/H grids. They have higher population density, and proportion of residential area, lower proportion of commercial area, and shorter distance to MTR stations. The L/L areas are scattered in the suburban areas or low-density residential areas of Hong Kong Island (e.g., Stanley), Kowloon (e.g., Yau Tong), and the New Territories (e.g., Sai Kung), often far away from city center. They have longer distance to MTR stations and city center, lower population density, proportion of residential area and proportion of commercial area.

5. Walking index

5.1. Definition

We believe that the spatial mismatch between the pedestrian demand and residential population can reveal the degree of walking attractiveness, i.e., to degree to which an area is conductive to walk. The distribution of residential population has a direct impact on collective walking behavior, e.g., pedestrian demand. Given other conditions are constant, an area with higher residential population will have higher pedestrian demand. Conversely, assuming equal population density between two areas, differences in pedestrian demand may reveal a difference in walking attractiveness. Furthermore, walking attractiveness may be different for certain groups of people, such as older or disabled pedestrians (Adkins et al., 2017; Forsyth et al., 2009; Frank et al., 2008; Lovasi et al., 2008). Therefore, we constructed a new walking index using the ratio of observed pedestrian demand of a given group and the residential population of that group with the following equation:

$$Walking\ Index_a^i = \frac{N_a^i}{P_a^i} \tag{1}$$

where N_a^i represents the number of pedestrians with attribute a in the i-th geographic unit, P_a^i represents the total residential population of

Table 3
The t-value of the t-test of built environment factors for four pairs of comparisons (H/H grids vs. non-H/H grids, L/H vs. non-L/H, H/L vs. non-H/L, L/L, vs. non-L/L in Fig. 8).

	Population density	Commercial proportion	Residential proportion	Distance to MTR	Distance to city center
H/H vs. non-H/H	10.02**	0.29	4.87**	−3.87**	−2.55**
L/H vs. non-L/H	−4.41**	4.99**	−3.20**	−0.10	−1.84**
H/L vs. non-H/L	4.41**	−1.50*	2.52**	−1.35*	1.07
L/L vs. non-L/L	−10.02**	−2.91**	−4.29**	5.19**	3.24*

* $p < 0.05$.
** $p < 0.01$.

people with attribute a in the i-th geographic unit.

The formula can be directly applied to older adults. The walking index for older adults (OWI) could be measured by the ratio of number of older pedestrians and population of older residents in an area. Similarly, it can also be used for other age groups, certain population subgroups, or all people.

To obtain the total population in customized units, we again collected data from WorldPop in 2020. We calculated the walking index for both older adults (OWI) and all people (WI) for the whole Hong Kong.

5.2. Distribution of walking index for older people (OWI)

We calculated the spatial distribution of OWI based on three spatial units: TPUs, 500 × 500 m rectangular grids and 200 × 200 m rectangular grids respectively. The results are visualized in Fig. 9(a)-(c). Of the ten TPUs with the highest OWI, three are in the northeast corner of the Central and Western District, four are in Tsim Sha Tsui and one is in Causeway Bay, which are the city center of Hong Kong where many shopping malls are located. Far away from city center, Sai Kung Peninsula also has a high OWI, which remains untouched by urbanization and is also a popular place for hiking. Of the ten TPUs with observed pedestrians and the lowest OWI, nine are scattered in New Territory.

5.3. Spatial mismatch between WI and OWI

This study mapped both WI and OWI in each 500 × 500 m rectangular grid in the same way. We classified all grids into high or low values of these two variables, according to their respective median value. Accordingly, we divided the grids into four groups: H/H (high WI and high OWI), H/L (low WI and high OWI), L/H (low WI and high OWI), and L/L (low WI and low OWI) (Fig. 10 and Table 4). In Table 5, we conducted t-tests for built environment features for four pairs of comparisons (H/H grids vs. non-H/H grids, L/H vs. non-L/H, H/L vs. non-H/L, L/L, vs. non-L/L in Fig. 10).

H/H areas are mainly concentrated in compact high and middle density residential areas such as Central District and Mong Kok. They have higher proportion of commercial area, lower proportion of residential area, population density, and shorter distance to city center, compared with other areas. L/H areas scatter around H/H areas especially in neighborhoods inhabited by affluent residents, such as the Mid-Levels. They have shorter distance to MTR stations. H/L areas are often dispersed throughout suburban and mountainous area with adequate green space. They have longer distance to MTR stations and city center, lower population density, proportion of residential area and the proportion of commercial area. L/L areas are mainly located at high and middle-rise residential area in New Territories and peripheries of Kowloon and Hong Kong Island especially in some new towns. They have higher population density and proportion of residential area, lower proportion of commercial area, and shorter distance to MTR stations,

5.4. The validation of WI and OWI

To validate the new walking index, we used data from the Hong Kong Travel Characteristics Survey (TCS) conducted by the Transport Department of the Hong Kong government in 2012. The data from TCS were acquired from a large representative sample of 101,385 residents in Hong Kong. The respondents were asked to provide individual information (e.g., age, gender, occupation, address) and trip information (e.g., trip mode, trip frequency) during the last 24 h up to the surveying time.

We ran two multivariate linear regressions to predict the WI (Model 1) and OWI (Model 3) and as independent variables (Table 6). As a comparison, we conducted two more models to predict frequency of walking trips of all respondents (Model 2) and older respondents (Model 4) with built environment factors. The unit of analysis is TPU for all models.

Built environment factors include population density (Barnett et al., 2017), street intersection density (Cerin, Nathan, Van Cauwenberg, Barnett, & Barnett, 2017), land-use diversity (Thornton et al., 2017), bus stop density (Christiansen et al., 2016), and the coverage of Mass transit rail (MRT) stations (Fenton, 2005). We geolocated all respondents in QGIS based on their dwelling locations. Population density was defined as the resident population per unit of area and obtained from Census and Statistics Department of Hong Kong. Street intersection density was defined as the number of street intersections per unit area. The land use

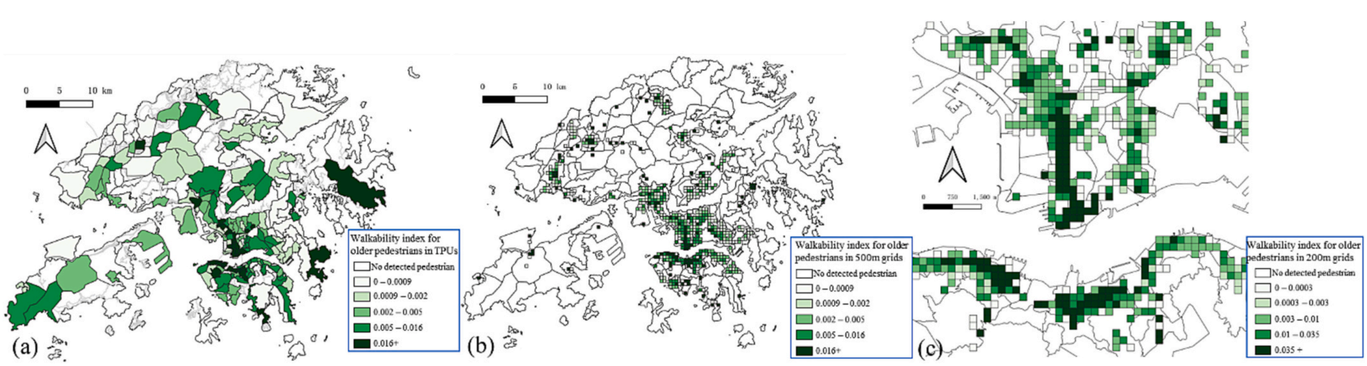

Fig. 9. Spatial distribution of OWI. (a) OWI at TPUs in Hong Kong; (b) OWI at 500 × 500 m rectangular grids in Hong Kong; (c) OWI at 200 × 200 m grids for the main area of Kowloon and Hong Kong Island.

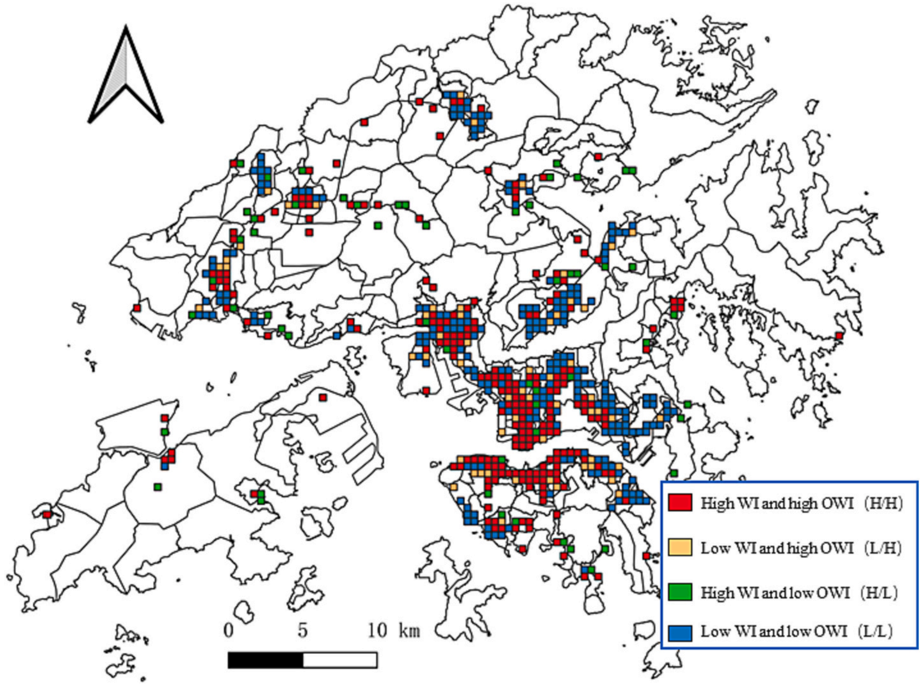

Fig. 10. Classification of urban areas into four groups, according to the proportion of older residents and the proportion of older detected pedestrians on SVI.

Table 4
Features and representative examples of four groups of areas in Fig. 9.

Type of area	Features	Representative location	Representative aerial view
High WI and high OWI (H/H)	Compact High and Mid-rise residential area	Central District, Mong Kok	
Low WI and high OWI (L/H)	Open High and Mid-rise residential area	Mid-levels, Quarry Bay	
High WI and low OWI (H/L)	Suburban and mountainous area	Lantau Island, Kam Tin	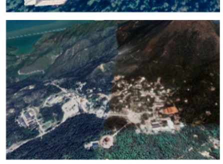
Low WI and low OWI (L/L)	High and Mid-rise residential area in New Territories and fringe of Kowloon and Hong Kong Island	Sha Tin, Chai Wan	

Source: Google Inc.

diversity was defined as the entropy score of land use distribution and calculated as $(-1)\sum_i(p_i ln(p_i))/ln(n)$, where p_i is the share of specific land use and n is the number of land use types. Bus stop density was calculated as the number of bus stops per unit of land area. The coverage of Mass Transit Railway (MTR) stations was defined as the percentage of land covered by the 500 m buffer of MTR stations. Both dependent variables and independent variables were converted into Z scores to obtain standardized coefficients, which allow us to compare the effect sizes of different factors in predicting the outcome.

Compared with average walking frequency from TCS, both WI and OWI have higher association with built-environment factors. Hence, our approach may better predict overall walking demand than traditional travel survey. It is worth noting that individual travel survey data may exhibit fluctuation due to the individual attributes of respondents. As such, the WI and OWI present a superior alternative to evaluate collective pedestrian activity.

6. Discussion

6.1. Methodological contribution

Previous studies have shown SVI to be a valuable data source for automatic and large-scale urban environment audits, with many focusing on static features such as buildings, roads, and greenery. Dynamic elements, including vehicles, pedestrians, and bicycles, have not been adequately studied primarily because of their volatility over time. Therefore, researchers typically measure pedestrian volumes and walking behavior through field observation or questionnaires. Field counts are time-, labor-, and cost-intensive, which is impractical for a large area (Lee & Talen, 2014). Self-reported data are prone to recall bias and may be difficult to be geolocated (Saelens & Handy, 2008).

Recently, some researchers have suggested that estimating pedestrian demand using SVI is feasible. The number of pedestrians at a given location at a given time can be estimated from a single SVI image. As the sample size increases exponentially (e.g., hundreds of SVIs at different locations and/or times in an area), the pedestrian volume estimate becomes closer to the true value for that area, although the estimate for a particular location or time may be very incorrect (Richards, 1961). Recent empirical studies have demonstrated the consistency of pedestrian volume between the estimate by SVI and the field audit, which reached 0.87 Cronbach's alpha under certain circumstances (Chen et al., 2020). This opened new possibilities for assessing pedestrian activity at a scale, depth, and scope inaccessible to traditional assessment methods.

In this study, we extend previous studies by developing a novel approach to assess pedestrian age groups in SVI. First, we used the existing pedestrian dataset RAP and PA -100 k as part of the training samples, which contain the age information to pre-train the models.

Table 5
The t-value of the t-test of built environment factors for four pairs of comparisons (H/H grids vs. non-H/H grids, L/H vs. non-L/H, H/L vs. non-H/L, L/L, vs. non-L/L in Fig. 10).

	Population density	Commercial proportion	Residential proportion	Distance to MTR	Distance to city center
H/H vs. non-H/H	−2.41**	4.58**	−2.25**	0.70	−2.14**
L/H vs. non-L/H	0.45	−0.83	0.18	−1.67**	−0.63
H/L vs. non-H/L	−4.38**	−1.48*	−1.90**	3.64**	2.72**
L/L vs. non-L/L	5.11**	−2.95**	3.55**	−2.16**	0.66

Note. *: $p < 0.05$; **: $p < 0.01$.

Table 6
Results of multivariate regression model of OWI and average walking frequency per older respondents from TCS with built-environment factors as independent variables.

	Model 1	Model 2	Model 3	Model 4
Dependent variable	WI	Walking frequency of all respondents	OWI	Walking frequency of older respondents
	Coef. (SE)	Coef. (SE)	Coef. (SE)	Coef. (SE)
Street intersection density	0.201 (0.069) **	−0.013 (0.011)	0.185 (0.059) *	−0.007 (0.005)
Population density	−0.292 (0.062) ***	−0.004 (0.011)	−0.202 (0.071) **	−0.004 (0.005)
Bus stop density	0.350 (0.083) ***	0.012 (0.005) *	0.347 (0.086) ***	0.024 (0.005) ***
MTR station 500 m coverage	0.283 (0.062) ***	0.040 (0.010) ***	0.213 (0.064) **	0.006 (0.004)
Land use diversity	0.175 (0.059) **	0.016 (0.011)	0.222 (0.061) ***	0.014 (0.004) **
Adjusted R^2	0.532	0.006	0.507	0.006

Note. *: $p < 0.05$; **: $p < 0.01$; ***: $p < 0.001$.

Second, we created our own training dataset based on SVI to refine the pre-trained model. After the two-stage training, the accuracy of the model tested on pruned SVIs reached 87.1%. Using this approach, we are able to identify older pedestrians in SVI. Our efforts can help create healthy cities and aging-friendly communities, which are critical for an aging society. It is also possible to use our approach to assess pedestrians of other age groups or specific attributes (e.g., female, or people using wheelchair).

More importantly, our approach also offers a unique advantage over traditional research studies. To assess the built environment's impact on travel behavior, traditional travel survey and research focused on built environment features around home. However, on average, Hong Kong people spend 40% of their waking time far away from home (Census and Statistics Department, C. and S. D, 2013). It has been pointed out that the uncertainty in identifying the spatial areas that influence individual behaviors may hinder our understanding of the environment-behavior link (Kwan, 2012). Therefore, to better understand the impact of built-environment context on walking behavior, we use the actual observed pedestrians to estimate walking demand in a given area.

Conventional environmental behavior research has typically employed travel surveys to obtain data on pedestrian walking patterns, specifically focusing on individual walking behavior. However, this study utilizes WI/OWI as a metric for assessing collective pedestrian activity on streets. We demonstrated that WI/OWI has a stronger correlation with the built environment features compared with individual walking behavior, which is in line with one previous study (Jiang et al., 2021). This also suggests that WI/OWI may serve as a more reliable measurement for evaluating walking environments, as opposed to travel surveys which are susceptible to the influence of personal attributes. Therefore, such an approach can advance the field of research by providing a much-needed spatial match between the built environment and collective pedestrian activity.

6.2. Spatial distribution of older pedestrian and OWI in Hong Kong

Using our new approach, we measured the spatial distribution of older pedestrians in Hong Kong. Several results are worth noting. First, there is an obvious spatial mismatch between older pedestrians and older residents. High number of older residents and high number of detected older pedestrians(H/H) grids concentrated in high-density compact development areas which are characterized by high-rise buildings and mixed land uses. These areas provide older residents with easy access to vital amenities, including healthcare, transportation, and commerce, situated within a walkable range, particularly addressing their mobility constraints (Burton, 2000). Low number of older residents and high number of detected older pedestrians(L/H) grids have built environment features similar to those of H/H areas, but with a high concentration of commercial destinations and fewer residential buildings. As a result, such built environments attract a large flow of older pedestrians living in other areas to fulfill utilitarian needs, such as going to a restaurant or visiting a doctor. These areas, such as Tsim Sha Tsui, Central District, often have high costs of living, which may exceed the affordability of older adults. High number of older residents and low number of detected older pedestrians (H/L) grids mainly scattered in low- and middle- density residential areas. Low number of older residents and low number of detected older pedestrians (L/L) areas are scattered in the suburban areas or low-density residential areas of Hong Kong Island (e.g., Stanley), Kowloon (e.g., Yau Tong), and the New Territories (e.g., Sai Kung). Both H/L and L/L areas are often far away from city center, and amenities, services, and healthcare facilities are scarce (Sun & Lau, 2021). The lack of walking destinations may hinder walking activities among older adults. Furthermore, residents living in those areas often have other transportation options, e.g., private vehicles, which partly reduce the need of walking.

To account for such spatial mismatch, we develop a new walking index for older people (OWI) based on the ratio of observed pedestrians to the resident population. It can reflect the quality of urban design, human activity, and urban vitality for older adults by measuring the extent to which they are willing to walk. Most studies quantify the walkability of a given area based on features of the built environment that support walking, such as the density of intersections, the continuity and directness of paths, and the presence of sidewalks and other pedestrian infrastructure (Chen, Lu, et al., 2022; Li et al., 2021; Yang et al., 2019). However, the availability and accessibility of pedestrian-friendly infrastructure may not reflect actual walking behavior in such an area. Our walking index can help fill this gap by accounting for collective walking behavior.

6.3. Spatial mismatch between WI and OWI

This study focuses on aging-friendly built environment and the pedestrian demand of older adults. Due to the unique needs and physical abilities of older pedestrians, locations that attract general pedestrians may not accommodate the older pedestrians. Therefore, we mapped the spatial mismatch between WI and OWI to explore the spatial disparity with four conditions (H/H, L/H, H/L, and L/L), and further identity the built environment features associated with each condition.

High WI and high OWI areas (H/H) are characterized by higher proportion of commercial area, lower proportion of residential area and a closer distance to the city center, compared with other areas. A high concentration of commercial spaces increases the availability of various services, shopping, dining, and entertainment options within walking distance. The areas close to the city center tend to have better pedestrian infrastructure, such as sidewalks, crosswalks, and street lighting, which enhances the safety and comfort of pedestrians. Low WI and high OWI (L/H) areas have shorter distances to MTR stations compared with other areas. This indicates that older adults are more sensitive to the accessibility of public transit compared with the general population. Accessibility to MTR is particularly appealing to older adults, because it is reliable, comfortable, and cost-effective (Hess, 2009; Kostyniuk & Shope, 2003) .

High WI and low OWI (H/L) areas are further away from MTR stations and the city center, and have lower proportions of commercial areas, compared with other areas. This further underscores the notion that older adults are more sensitive to the accessibility of commercial destinations and public transport. Low WI and low OWI areas (L/L) are featured by higher population density and proportion of residential area, a lower proportion of commercial, and further away from the city center, compared with others. Most of these areas are high-density housing estates featuring multiple high-rise residential buildings in New Territories and the fringe of Kowloon and Hong Kong Island. The lack of commercial facilities and dense living environment may hinder the older adults' willingness to walk.

6.4. Limitations and future research

Based on this study, four possible directions for future research emerge. First, this study has identified associations between older pedestrian count and built environment factors. However, more rigorous research designs (e.g., natural experiments) are necessary to find out any causal relationships between pedestrian volume, built-environment factors and older adults' willingness to walk. Second, pedestrian behavior can be measured using individual-level mobility data extracted from mobile data to understand individual walking behavior and its geographic context. Third, other attributes of pedestrians such as gender and disability are also meaningful and should receive more attention. Fourth, population-weighted exposure and the Gini index of exposure of different groups of people to the built environment can be further investigated.

7. Conclusion

In this study, we proposed a novel approach to automatically recognize older adults using SVI, which could be used to estimate pedestrian demand and evaluate the walking environment for older people. Our proposed model achieved high accuracy (87.1%) in detecting older pedestrians from SVIs. The results of the multivariate regression models illustrated that the ratio of older pedestrians to older residents has the potential to be a good indicator of walking attractiveness for older adults, especially in high residential areas. The result also indicated a spatial mismatch between the walking and resident population for older people. Researchers and urban planners should consider the distribution and needs of older pedestrians for further urban planning interventions.

Funding

The work described in this paper was fully supported by the Research Grants Council of the Hong Kong SAR (Project No. CityU11207520).

Declaration of Competing Interest

The authors declare that they have no known competing financial interests or personal relationships that could have appeared to influence the work reported in this paper.

Data availability

No data was used for the research described in the article.

References

Adkins, A., Makarewicz, C., Scanze, M., Ingram, M., & Luhr, G. (2017). Contextualizing walkability: Do relationships between built environments and walking vary by socioeconomic context? *Journal of the American Planning Association, 83*(3), 296–314.

Aune, D., Sen, A., Henriksen, T., Saugstad, O. D., & Tonstad, S. (2016). Physical activity and the risk of gestational diabetes mellitus: A systematic review and dose–response meta-analysis of epidemiological studies. *European Journal of Epidemiology, 31*(10), 967–997.

Barnett, D. W., Barnett, A., Nathan, A., Van Cauwenberg, J., & Cerin, E. (2017). Built environmental correlates of older adults' total physical activity and walking: A systematic review and meta-analysis. *International Journal of Behavioral Nutrition and Physical Activity, 14*(1), 1–24.

Bennie, J. A., Chau, J. Y., van der Ploeg, H. P., Stamatakis, E., Do, A., & Bauman, A. (2013). The prevalence and correlates of sitting in European adults-a comparison of 32 Eurobarometer-participating countries. *International Journal of Behavioral Nutrition and Physical Activity, 10*(1), 1–13.

Boyle, T., Keegel, T., Bull, F., Heyworth, J., & Fritschi, L. (2012). Physical activity and risks of proximal and distal colon cancers: A systematic review and meta-analysis. *Journal of the National Cancer Institute, 104*(20), 1548–1561.

Brownson, R. C., Hoehner, C. M., Day, K., Forsyth, A., & Sallis, J. F. (2009). Measuring the built environment for physical activity: State of the science. *American Journal of Preventive Medicine, 36*(4), S99–S123 (e12).

Burton, E. (2000). The compact city: Just or just compact? A preliminary analysis. *Urban Studies, 37*(11), 1969–2006.

Carr, L. J., Dunsiger, S. I., & Marcus, B. H. (2010). Walk scoreTM as a global estimate of neighborhood walkability. *American Journal of Preventive Medicine, 39*(5), 460–463.

Census and Statistics Department. (2020). *Hong Kong population projections 2020-2069*. Census and Statistics Department. https://www.statistics.gov.hk/pub/B1120015082020XXXXB0100.pdf.

Census and Statistics Department, C. and S. D. (2013). *Thematic Household Survey Report—Report No. 56*.

Cerin, E., Lee, K., Barnett, A., Sit, C. H. P., Cheung, M., & Chan, W. (2013). Objectively-measured neighborhood environments and leisure-time physical activity in Chinese urban elders. *Preventive Medicine, 56*(1), 86–89. https://doi.org/10.1016/j.ypmed.2012.10.024

Cerin, E., Nathan, A., Van Cauwenberg, J., Barnett, D. W., & Barnett, A. (2017). The neighbourhood physical environment and active travel in older adults: A systematic review and meta-analysis. *International Journal of Behavioral Nutrition and Physical Activity, 14*(1), 1–23.

Chen, B., Tu, Y., Wu, S., Song, Y., Jin, Y., Webster, C., Xu, B., & Gong, P. (2022). Beyond green environments: Multi-scale difference in human exposure to greenspace in China. *Environment International, 166*, Article 107348.

Chen, L., Lu, Y., Sheng, Q., Ye, Y., Wang, R., & Liu, Y. (2020). Estimating pedestrian volume using street view images: A large-scale validation test. *Computers, Environment and Urban Systems, 81*, Article 101481.

Chen, L., Lu, Y., Ye, Y., Xiao, Y., & Yang, L. (2022). Examining the association between the built environment and pedestrian volume using street view images. *Cities, 103734*.

Chen, S., Wang, T., Bao, Z., & Lou, V. (2022). A path analysis of the effect of neighborhood built environment on public health of older adults: A Hong Kong study. *Frontiers in Public Health, 10*.

Chodzko-Zajko, W. J., Proctor, D. N., Singh, M. A. F., Minson, C. T., Nigg, C. R., Salem, G. J., & Skinner, J. S. (2009). Exercise and physical activity for older adults. *Medicine & Science in Sports & Exercise, 41*(7), 1510–1530.

Christiansen, L. B., Cerin, E., Badland, H., Kerr, J., Davey, R., Troelsen, J., … Sugiyama, T. (2016). International comparisons of the associations between objective measures of the built environment and transport-related walking and cycling: IPEN adult study. *Journal of Transport & Health, 3*(4), 467–478.

Deng, Y., Luo, P., Loy, C. C., & Tang, X. (2014). Pedestrian attribute recognition at far distance. In *Proceedings of the 22nd ACM international conference on multimedia* (pp. 789–792).

Dhanani, A., Tarkhanyan, L., & Vaughan, L. (2017). Estimating pedestrian demand for active transport evaluation and planning. *Transportation Research Part A: Policy and Practice, 103*, 54–69.

Dovey, K., & Pafka, E. (2020). What is walkability? The urban DMA. *Urban Studies, 57*(1), 93–108.

Du, Y., Yue, J., Ji, Y., & Sun, L. (2017). Exploration of optimal Wi-fi probes layout and estimation model of real-time pedestrian volume detection. *International Journal of Distributed Sensor Networks, 13*(11), 1550147717741857.

Feng, J. (2017). The influence of built environment on travel behavior of the elderly in urban China. *Transportation Research Part D: Transport and Environment, 52*, 619–633.

Fenton, M. (2005). Battling America's epidemic of physical inactivity: Building more walkable, livable communities. *Journal of Nutrition Education and Behavior, 37*, S115–S120.
Forsyth, A. (2015). What is a walkable place? The walkability debate in urban design. *Urban Design International, 20*(4), 274–292.
Forsyth, A., Oakes, J. M., Lee, B., & Schmitz, K. H. (2009). The built environment, walking, and physical activity: Is the environment more important to some people than others? *Transportation Research Part D: Transport and Environment, 14*(1), 42–49.
Frank, L. D., Kerr, J., Sallis, J. F., Miles, R., & Chapman, J. (2008). A hierarchy of sociodemographic and environmental correlates of walking and obesity. *Preventive Medicine, 47*(2), 172–178.
Ghani, F., Rachele, J. N., Loh, V. H., Washington, S., & Turrell, G. (2018). Do differences in built environments explain age differences in transport walking across neighbourhoods? *Journal of Transport & Health, 9*, 83–95.
Habibzadeh, M., Jannesari, M., Rezaei, Z., Baharvand, H., & Totonchi, M. (2018). Automatic white blood cell classification using pre-trained deep learning models: Resnet and inception. In *, 10696. Tenth international conference on machine vision (ICMV 2017)* (pp. 274–281).
Harvey, J. A., Chastin, S. F., & Skelton, D. A. (2015). How sedentary are older people? A systematic review of the amount of sedentary behavior. *Journal of Aging and Physical Activity, 23*(3).
Hess, D. B. (2009). Access to public transit and its influence on ridership for older adults in two US cities. *Journal of Transport and Land Use, 2*(1), 3–27.
Hidayati, S. C., You, C.-W., Cheng, W.-H., & Hua, K.-L. (2017). Learning and recognition of clothing genres from full-body images. *IEEE Transactions on Cybernetics, 48*(5), 1647–1659.
Huang, G., Li, D., Yu, L., Yang, D., & Wang, Y. (2022). Factors affecting sustainability of smart city services in China: From the perspective of citizens' sense of gain. *Habitat International, 128*, Article 102645.
Hui, S. C., Chan, C. M., Wong, S. H. S., Ha, A. S. C., & Hong, Y. L. (2001). Physical activity levels of Chinese youths and the association with physical fitness and demographic variables: The Hong Kong youth fitness study. *Research Quarterly for Exercise and Sport, 72*(1), A92–A93.
Husni, M., & Suryana, N. (2010). Crowd event detection in computer vision. In *, 1. 2010 2nd International Conference on Signal Processing Systems*. V1-444-V1-447.
Jiang, Y., Chen, L., Grekousis, G., Xiao, Y., Ye, Y., & Lu, Y. (2021). Spatial disparity of individual and collective walking behaviors: A new theoretical framework. *Transportation Research Part D: Transport and Environment, 101*, Article 103096.
Kamada, M., Kitayuguchi, J., Shiwaku, K., Inoue, S., Okada, S., & Mutoh, Y. (2011). Differences in association of walking for recreation and for transport with maximum walking speed in an elderly Japanese community population. *Journal of Physical Activity and Health, 8*(6), 841–847.
Koonce, B. (2021). ResNet 50. In *Convolutional neural networks with swift for tensorflow* (pp. 63–72). Springer.
Kostyniuk, L. P., & Shope, J. T. (2003). Driving and alternatives: Older drivers in Michigan. *Journal of Safety Research, 34*(4), 407–414.
Kwan, M.-P. (2012). The uncertain geographic context problem. *Annals of the Association of American Geographers, 102*(5), 958–968.
Lee, I.-M., Shiroma, E. J., Lobelo, F., Puska, P., Blair, S. N., Katzmarzyk, P. T., & Group, L. P. A. S. W. (2012). Effect of physical inactivity on major non-communicable diseases worldwide: An analysis of burden of disease and life expectancy. *The Lancet, 380* (9838), 219–229.
Lee, S., Sung, H., & Woo, A. (2017). The spatial variations of relationship between built environment and pedestrian volume: Focused on the 2009 Seoul pedestrian flow survey in Korea. *Journal of Asian Architecture and Building Engineering, 16*(1), 147–154.
Lee, S., & Talen, E. (2014). Measuring walkability: A note on auditing methods. *Journal of Urban Design, 19*(3), 368–388.
Li, D., Zhang, Z., Chen, X., & Huang, K. (2018). A richly annotated pedestrian dataset for person retrieval in real surveillance scenarios. *IEEE Transactions on Image Processing, 28*(4), 1575–1590.
Li, S., Ma, S., Tong, D., Jia, Z., Li, P., & Long, Y. (2021). Associations between the quality of street space and the attributes of the built environment using large volumes of street view pictures. *Environment and Planning B: Urban Analytics and City Science, 49* (4), 1197–1211.
Liang, R., Zhu, Y., & Wang, H. (2014). Counting crowd flow based on feature points. *Neurocomputing, 133*, 377–384.
Lin, T.-Y., Maire, M., Belongie, S., Hays, J., Perona, P., Ramanan, D., … Zitnick, C. L. (2014). Microsoft coco: Common objects in context. *European Conference on Computer Vision*, 740–755.
Liu, D., Jiang, Y., Wang, R., & Lu, Y. (2023). Establishing a citywide street tree inventory with street view images and computer vision techniques. *Computers, Environment and Urban Systems, 100*, Article 101924. https://doi.org/10.1016/j.compenvurbsys.2022.101924
Liu, W., Anguelov, D., Erhan, D., Szegedy, C., Reed, S., Fu, C.-Y., & Berg, A. C. (2016). Ssd: Single shot multibox detector. *European Conference on Computer Vision*, 21–37.
Liu, X., Zhao, H., Tian, M., Sheng, L., Shao, J., Yi, S., Yan, J., & Wang, X. (2017). Hydraplus-net: Attentive deep features for pedestrian analysis. *Proceedings of the IEEE International Conference on Computer Vision*, 350–359.
Long, Y., & Thill, J.-C. (2015). Combining smart card data and household travel survey to analyze jobs–housing relationships in Beijing. *Computers, Environment and Urban Systems, 53*, 19–35.
Lovasi, G. S., Quinn, J. W., Neckerman, K. M., Perzanowski, M. S., & Rundle, A. (2008). Children living in areas with more street trees have lower prevalence of asthma. *Journal of Epidemiology & Community Health, 62*(7), 647–649.
Lu, Y. (2019). Using Google street view to investigate the association between street greenery and physical activity. *Landscape and Urban Planning, 191*, Article 103435.
Luo, S., Xie, J., & Furuya, K. (2022). Using Google street view panoramas to evaluate the environmental aesthetics quality of blue spaces in urban area. *IOP Conference Series: Earth and Environmental Science, 1092*(1), Article 012001.
Manson, J. E., Hu, F. B., Rich-Edwards, J. W., Colditz, G. A., Stampfer, M. J., Willett, W. C., … Hennekens, C. H. (1999). A prospective study of walking as compared with vigorous exercise in the prevention of coronary heart disease in women. *New England Journal of Medicine, 341*(9), 650–658.
Mendes de Leon, C. F., Cagney, K. A., Bienias, J. L., Barnes, L. L., Skarupski, K. A., Scherr, P. A., & Evans, D. A. (2009). Neighborhood social cohesion and disorder in relation to walking in community-dwelling older adults: A multilevel analysis. *Journal of Aging and Health, 21*(1), 155–171.
Moniruzzaman, M., Páez, A., Scott, D., & Morency, C. (2015). Trip generation of seniors and the geography of walking in Montreal. *Environment and Planning A: Economy and Space, 47*(4), 957–976.
Ning, H., Ye, X., Chen, Z., Liu, T., & Cao, T. (2022). Sidewalk extraction using aerial and street view images. *Environment and Planning B: Urban Analytics and City Science, 49* (1), 7–22.
Ogawa, M., & Aizawa, K. (2019). Identification of buildings in street images using map information. *IEEE International Conference on Image Processing (ICIP), 2019*, 984–988.
Organization, W. H. (2007). *Checklist of essential features of age-friendly cities*. World Health Organization.
Pahor, M., Guralnik, J. M., Ambrosius, W. T., Blair, S., Bonds, D. E., Church, T. S., … for the LIFE study investigators.. (2014). Effect of structured physical activity on prevention of major mobility disability in older adults: The LIFE study randomized clinical trial. *JAMA, 311*(23), 2387–2396. https://doi.org/10.1001/jama.2014.5616
Redmon, J., Divvala, S., Girshick, R., & Farhadi, A. (2016). You only look once: Unified, real-time object detection. In *Proceedings of the IEEE Conference on Computer Vision and Pattern Recognition* (pp. 779–788).
Redmon, J., & Farhadi, A. (2017). YOLO9000: Better, faster, stronger. In *Proceedings of the IEEE Conference on Computer Vision and Pattern Recognition* (pp. 7263–7271).
Ren, S., He, K., Girshick, R., & Sun, J. (2015). Faster r-cnn: Towards real-time object detection with region proposal networks. *Advances in Neural Information Processing Systems, 28*.
de Rezende, L. F. M., Rodrigues Lopes, M., Rey-López, J. P., Matsudo, V. K. R., Luiz, O., & do C.. (2014). Sedentary behavior and health outcomes: An overview of systematic reviews. *PLoS One, 9*(8), Article e105620.
Richards, F. S. (1961). A method of maximum-likelihood estimation. *Journal of the Royal Statistical Society: Series B: Methodological, 23*(2), 469–475.
Rodriguez, M., Laptev, I., Sivic, J., & Audibert, J.-Y. (2011). Density-aware person detection and tracking in crowds. *International Conference on Computer Vision, 2011*, 2423–2430.
Saelens, B. E., & Handy, S. L. (2008). Built environment correlates of walking: A review. *Medicine and Science in Sports and Exercise, 40*(7 Suppl), S550.
Saxena, S., Brémond, F., Thonnat, M., & Ma, R. (2008). Crowd behavior recognition for video surveillance. *International Conference on Advanced Concepts for Intelligent Vision Systems*, 970–981.
Schwartz, W. (2000). *Bicycle and pedestrian data: Sources, needs, and gaps*.
Shigematsu, R., Sallis, J. F., Conway, T. L., Saelens, B. E., Frank, L. D., Cain, K. L., … King, A. C. (2009). Age differences in the relation of perceived neighborhood environment to walking. *Medicine and Science in Sports and Exercise, 41*(2), 314.
Shorten, C., & Khoshgoftaar, T. M. (2019). A survey on image data augmentation for deep learning. *Journal of Big Data, 6*(1), 1–48.
Smith, T. C., Wingard, D. L., Smith, B., Kritz-Silverstein, D., & Barrett-Connor, E. (2007). Walking decreased risk of cardiovascular disease mortality in older adults with diabetes. *Journal of Clinical Epidemiology, 60*(3), 309–317.
Stevens, F. R., Gaughan, A. E., Linard, C., & Tatem, A. J. (2015). Disaggregating census data for population mapping using random forests with remotely-sensed and ancillary data. *PloS one, 10*(2), Article e0107042.
Sun, G., & Lau, C. Y. (2021). Go-along with older people to public transport in high-density cities: Understanding the concerns and walking barriers through their lens. *Journal of Transport & Health, 21*, Article 101072.
Sung, H., Lee, S., & Cheon, S. (2015). Operationalizing jane jacobs's urban design theory: Empirical verification from the great city of Seoul, Korea. *Journal of Planning Education and Research, 35*(2), 117–130.
Thom, N., & Hand, E. M. (2020). Facial attribute recognition: A survey. *Computer Vision: A Reference Guide*, 1–13.
Thornton, C. M., Kerr, J., Conway, T. L., Saelens, B. E., Sallis, J. F., Ahn, D. K., … King, A. C. (2017). Physical activity in older adults: An ecological approach. *Annals of Behavioral Medicine, 51*(2), 159–169.
Tsunoda, K., Tsuji, T., Kitano, N., Mitsuishi, Y., Yoon, J.-Y., Yoon, J., & Okura, T. (2012). Associations of physical activity with neighborhood environments and transportation modes in older Japanese adults. *Preventive Medicine, 55*(2), 113–118.
Van Holle, V., Van Cauwenberg, J., Gheysen, F., Van Dyck, D., Deforche, B., Van de Weghe, N., & De Bourdeaudhuij, I. (2016). The association between Belgian older adults' physical functioning and physical activity: What is the moderating role of the physical environment? *PLoS One, 11*(2), Article e0148398.
Wang, R., Yuan, Y., Liu, Y., Zhang, J., Liu, P., Lu, Y., & Yao, Y. (2019). Using street view data and machine learning to assess how perception of neighborhood safety influences urban residents' mental health. *Health & Place, 59*, Article 102186.
Wang, X., Zheng, S., Yang, R., Zheng, A., Chen, Z., Tang, J., & Luo, B. (2022). Pedestrian attribute recognition: A survey. *Pattern Recognition, 121*, Article 108220.
Weiss, K., Khoshgoftaar, T. M., & Wang, D. (2016). A survey of transfer learning. *Journal of Big Data, 3*(1), 1–40.

Wichrowska, O., Maheswaranathan, N., Hoffman, M. W., Colmenarejo, S. G., Denil, M., Freitas, N., & Sohl-Dickstein, J. (2017). Learned optimizers that scale and generalize. *International Conference on Machine Learning*, 3751–3760.

Wu, S., Moore, B. E., & Shah, M. (2010). Chaotic invariants of lagrangian particle trajectories for anomaly detection in crowded scenes. *IEEE Computer Society Conference on Computer Vision and Pattern Recognition, 2010*, 2054–2060.

Wu, Y., Zhang, D., & Kang, S. (2013). Physical activity and risk of breast cancer: A meta-analysis of prospective studies. *Breast Cancer Research and Treatment, 137*(3), 869–882.

Xiang, J., Dong, T., Pan, R., & Gao, W. (2020). Clothing attribute recognition based on RCNN framework using L-Softmax loss. *IEEE Access, 8*, 48299–48313.

Yang, Y., He, D., Gou, Z., Wang, R., Liu, Y., & Lu, Y. (2019). Association between street greenery and walking behavior in older adults in Hong Kong. *Sustainable Cities and Society, 51*, Article 101747.

Yin, L. (2017). Street level urban design qualities for walkability: Combining 2D and 3D GIS measures. *Computers, Environment and Urban Systems, 64*, 288–296.

Yin, L., Cheng, Q., Wang, Z., & Shao, Z. (2015). Big data'for pedestrian volume: Exploring the use of Google street view images for pedestrian counts. *Applied Geography, 63*, 337–345.